https://dx.doi.org/10.4314/dujopas.v8i2b.14
ISSN (Print): 2476-8316
ISSN (Online): 2635-3490
Dutse Journal of Pure and Applied Sciences (DUJOPAS), *Vol. 8 No. 2b June 2022*

Determination of Heat Flow and Temperature Variations for Geothermal Energy Assessment over Sokoto Basin, Nigeria, using Aero-Magnetic and Aero-Radiometric Data

Yakubu, M.B.[1], Lawal K.M.[1], Dewu B.B.M.[2], Ikpokonte A.E.[3]

[1] Department of Physics,
Ahmadu Bello University, Zaria

[2]Centre for Energy Research and Training,
Ahmadu Bello University, Zaria

[3]Department of Geology,
Ahmadu Bello University, Zaria

Email: bashaish12@gmail.com

Abstract

The Nigerian sector of Iullemmeden Basin (Sokoto Basin and its adjacent region) contains sediments between the ages of Cretaceous and Tertiary covering the entire Basin. The area is bounded by latitude 12° 5' – 14°00''N and longitude 4°00'' – 7°00''E. The study investigates geothermal energy resource potential over the Sokoto Basin using aeromagnetic and radiometric data. Seventeen (17) blocks of aeromagnetic and aero-radiometric data were gridded and processed using dimension of 55 km x 55 km. Spectral centroid method was employed to approximate depths to top and centroid of the magnetic sources of the study area. The results divulge that values of CPD range from 5.0 km to 12.5 km having a mean value of 8.8 km, whereby, the values of geothermal gradient range from 46.4 $^{o}Ckm^{-1}$ to 116.9 $^{o}Ckm^{-1}$ having a mean value of 81.6 $^{o}Ckm^{-1}$, while the values of heat flow range from 115.9 mWm^{-2} to 292.1 mWm^{-2} having a mean value of 204.1 mWm^{-2}. The study also reveals that, the values of radiogenic heat range between 0.81 and 2.87 μWm^{-3}. The zones having high concentration of thorium and uranium trending N-S and S-W extend to Niger Republic across mid-northern border. The result from this study also reveals that, Curie temperature could be attained at the depth of 6 km deep. Conclusively, those spots having shallow CPD and high heat flow may be potential for geothermal energy source.

Keywords: Radiogenic heat generation, Heat flow, Temperature variation, Curie point depths, Geothermal energy

INTRODUCTION

Temperature as a driven parameter in identifying geothermal energy resource potential zones in the earth's crust differs and these distinctions depend on the geology and activities that had taken place within geologic ages. The heat emanated from these temperature variations may perhaps come as a result of magnetic anomalies and/or radio-elements concentration of potassium, uranium and/or thorium released through the radioactive decay of its isotopes.

**Author for Correspondence*

Geothermal resource (energy) is a natural source of heat generated within the earth subsurface which is stored in a fractured rock's unit (reservoir) in a form of hot water or steam. The resources can be extracted and utilize for heating and/or convert it into electric power. Thus, aeromagnetic and airborne radiometric data may well be employed to reduce noise, enhance the data and/or integrate by means of other geophysical data (Megwara *et al*., 2013).

Recently, geophysical investigation especially from works of Megwara (2013); Nwankwo & Shehu (2015); Olorunsola & Chukwu (2018); Ezekiel (2019); Olorunsola & Aigbogun (2017); Yakubu *et al*. (2022); Saada (2016); Quintero *et al*. (2019); showed immense potential for geothermal energy source and radiogenic heat generation within Sokoto, Bida, southern Anambra Basin, Kano, Nigeria, NW desert Egypt and Colombian Caribbean (NW South America) respectively, by estimating the Curie point depths to derive other important geothermal parameters such as heat flow and/or geothermal gradient in their respective areas of study.

Moreover, Curie-point depths (CPD) were determined from magnetic data by either spectral analyses method (Okubo *et al.,* 1985) or any other statistical methods. The depths to Curie point may be deep or shallow depending on heat flow and/or composition of the rock type. Thus, 580 °C was considered as the Curie temperature for magnetite within the earth's crust since magnetite is the majority magnetic mineral therein (Tanaka *et al*., 1999).

In addition to the magnetic anomalies, the heat within the upper crust may well be estimated using radiometric data of radio-element such as U, Th and/or K (Keary *et al.,* 2002).

This study, estimates radiogenic heat generation, CPD, geothermal gradient, heat flow and temperature variation with depths to analyze the geothermal potential within the Sokoto Basin and its adjacent region covering sectors of the Iullemmeden Basin within Nigeria using aeromagnetic and aero- radiometric data of the study area. These data were acquired by Fugro between the year of 2003 and 2010 for Nigerian Geological Survey Agency (NGSA).

Thus, to my awareness, no work of this nature within the study area combines these parameters (especially, temperature variation with depths).

The area is bounded by latitude 12° 5' – 14°00''N and longitude 4°00'' – 7°00''E. Geologically, Sokoto Basin (see figure 1) contains sediments between the ages of Cretaceous and Tertiary is also called the Nigerian sector of the Iullemmeden Basin (Kogbe, 1981; Obaje, 2009). These sediments thicken and dip gently slowly towards the NW, having maximum thickness greater than 1200 m which trend close to the boundary of Niger Republic.

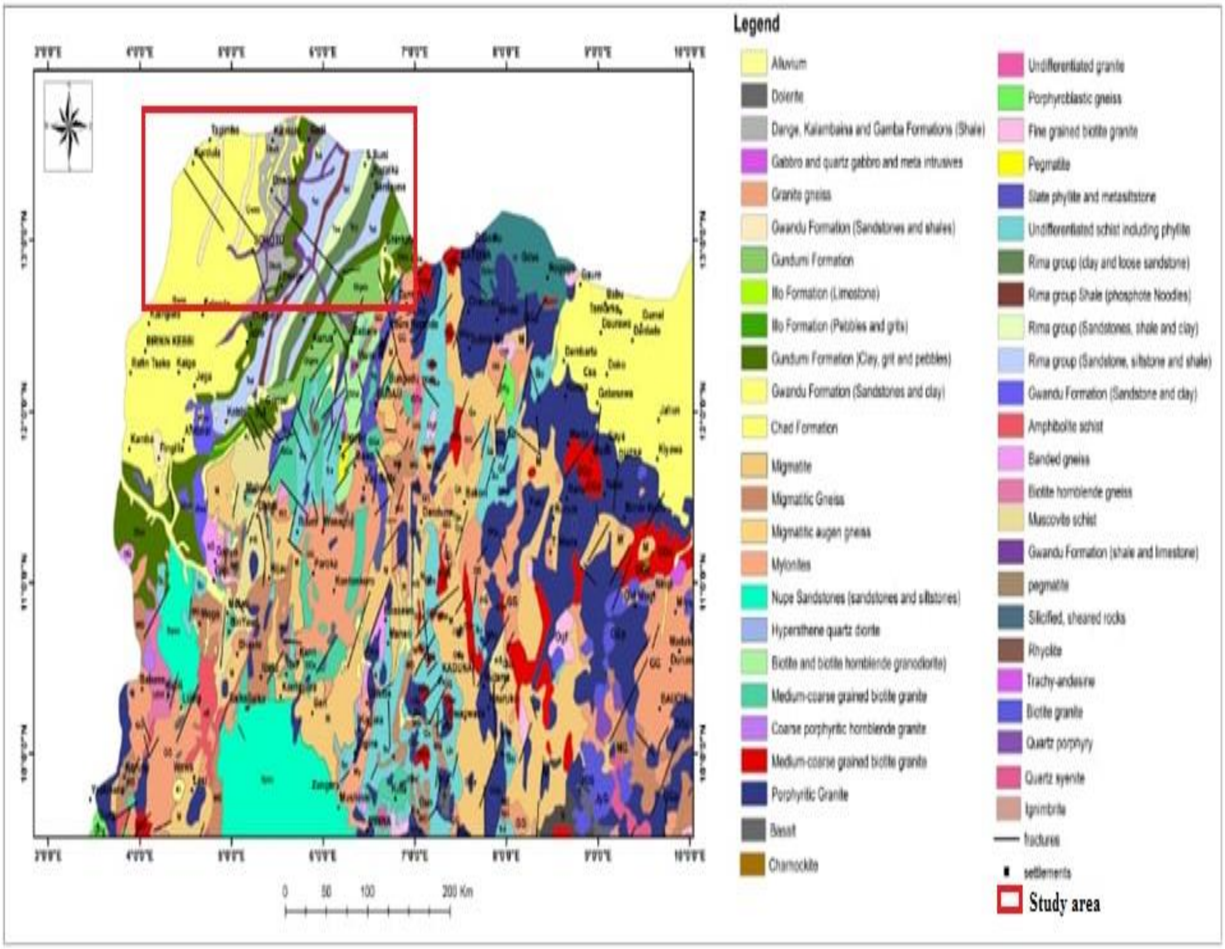

Figure 1: Geological map of North-western Nigeria showing the study area (after NGSA, 2004)

MATERIALS AND METHOD

The study begins with obtaining the necessary materials needed as follow:

Acquisition and Processing of Data

The aeromagnetic (HRAM) data was acquired through a Survey conducted between 2003 and 2010 by Fugro using seven Cessna Caravan fixed-wing aircraft with each aircraft carrying three Scintrex Cesium vapor magnetometers. The survey carried out on row spacing of 500 m having average topographic gap of 80 m, which gives about 2 million row-km of data. The data sorting interval was 0.1 seconds and/or less than 7 minutes. The acquired data by Fugro was pile up in the following format; 'X' column represents longitude/easting, 'Y' column represents latitude/northing, and 'Z' column represents total field magnetic intensity (TMI, in nT). Thus, columns X and Y were geo-referenced in the UTM projection system and considered as the preferred columns. However, in order to produce the total magnetic field (TMI) of the study area, the datasets were gridded by employs projection technique using Universal Transverse Mercator (UTM) and WGS 84 as orientation to obtained the seventeen (17) blocks of the magnetic data (figure 2) with a dimension of 55×55 km window size.

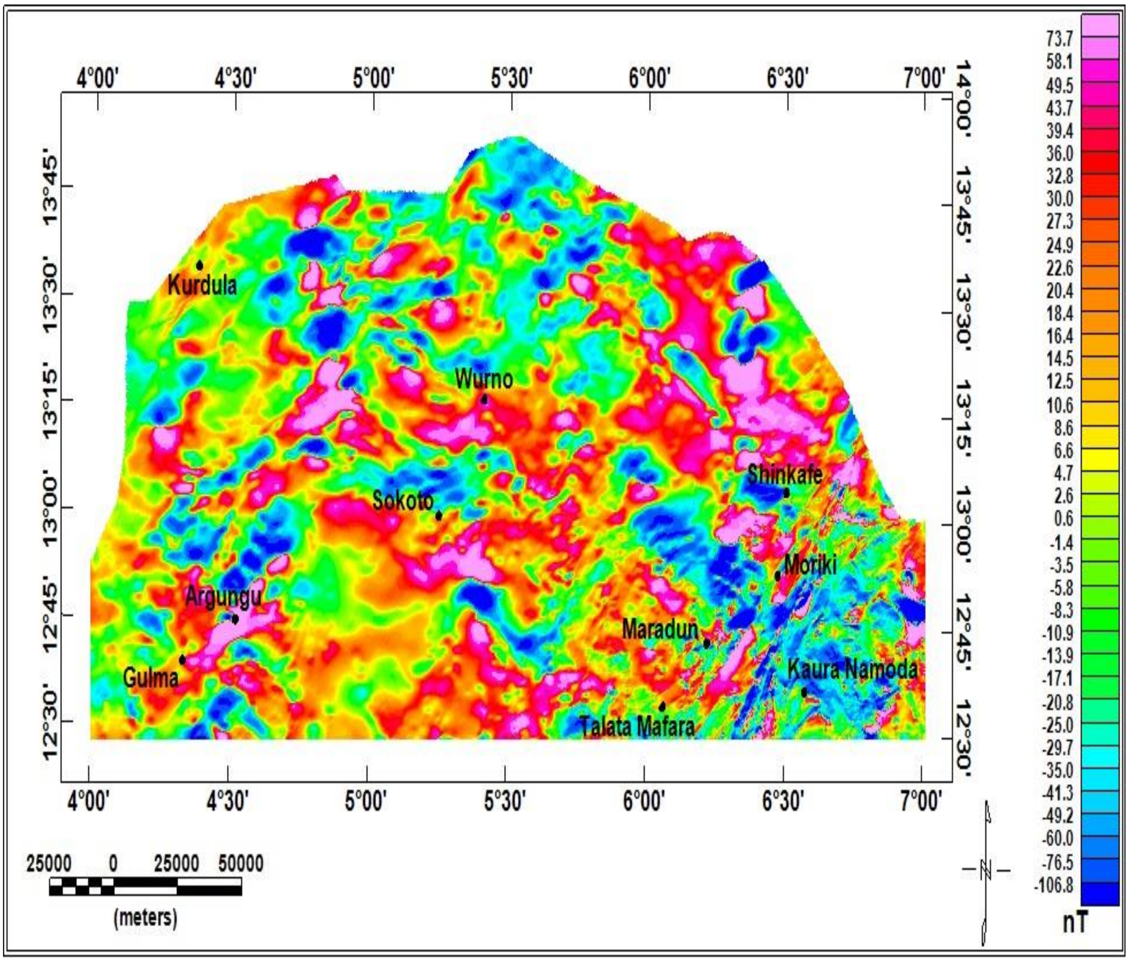

Figure 2: Map of Residual Magnetic field of the study area.

The 17 blocks of the gridded data (Figure 2) were also processed using different techniques such as regional-residual separation (figure 2 and 3), tapering, fast-Fourier transform and zero-padding. Then spectral centroid technique was applied on the processed data to estimate the CPD using Oasis Montaj software.

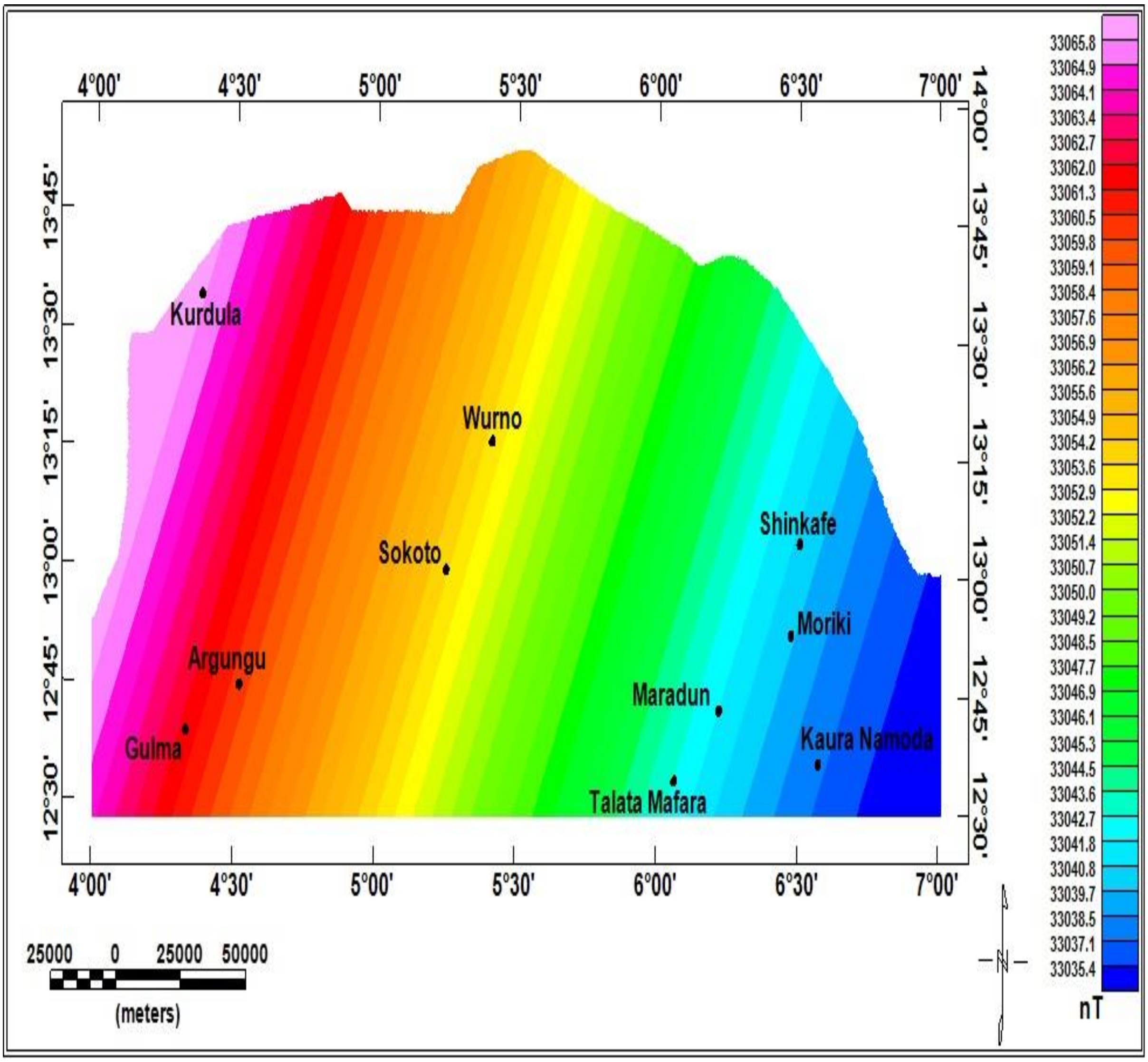

Figure 3: Map of Regional Magnetic field of the study area.

Table 1: Thermal Conductivities and Densities of Common Rocks in the Study Area (After Horai, 1971; Cermak & Rybach, 1982)

ROCK TYPES	RANGES OF THERMAL CONDUCTIVITY (W/m°C)	RANGES OF DENSITY	MEAN VALUES OF THERMAL CONDUCTIVITY (W/m°C)	MEAN VALUES OF DENSITY g/cm³
Quartz	0.89 – 2.03	2.34 -2.96	1.46	2.65
Shale	1.05 – 1.45	2.08 – 2.78	1.25	2.43
Migmatite	2.39 – 3.41	2.43 – 287	2.9	2.65
Granite	1.9 – 3.2	2.55 – 2.74	2.55	2.65
Silicate	2.41-3.39	1.98 – 3.32	2.9	2.65
Clay	1.38 - 2.70	0.90 – 1.50	2.04	1.2
Sandstone	2.5 – 3.2	2.0 – 2.6	2.85	2.85
Limestone	2.50 – 3.23	2.20 – 3.14	2.85	2.7
Schist	0.25 – 2.8	2.64 – 2.88	1.53	2.76
Alluvium	1.38 – 2.70	0.90 – 1.50	2.04	1.2
Gneiss	0.94 – 4.86	2.57 – 2.88	2.9	2.65
Dolorite	1.92 -2.72	2.83 – 3.07	2.32	2.95

METHODOLOGY

The Spectral analysis method was used to estimate Curie point depths (CPD) of each of the 17 blocks of the processed magnetic data for the assessment of the geothermal potential over the area of study. Though different approaches exist but to achieve the estimation of depth to the bottom of magnetic sources by estimating depths to the top and centroid; the centroid technique is the most commonly used, because it presents better results for depths estimation with less errors in contrast with other methods (Ravat *et al.*, 2007). This approach was also adopted in this work. The centoid method is based on mathematical evaluation of the shape of isolated magnetic anomalous body buried in the earth's crust and statistical properties of magnetic bodies (Bhattacharyya & Leu 1975; Spector & Grant 1970).

The depth to the centroid of the magnetic source is estimated using the low wave number and /or high wave length part of the power spectrum given in equation 1:

$$\frac{\ln(P(k)^{1/2}}{k} = \mathcal{A} - |k|Z_{\circ} \qquad 1$$

where, k is wave number, $\mathcal{A}$ is a constant and $Z_{\circ}$ is the centroid depth and $\boldsymbol{P}(k)$ is power spectrum.

Likewise, the depth to the top of the magnetic sources was derived from the slope of the medium to low wave length and/or high wave number portion of the power spectrum as expressed in equation 2:

$$\ln(\,P(k)^{1/2} \;= \mathcal{B} - |k|Z_t \qquad 2$$

where, Z_t is depth to the top of magnetic sources and $\mathcal{B}$ is a constant. The depth to the bottom (CPD) of the magnetic source (Z_b) is obtained from the relation in equation 3 (Okubo *et al.*, 1985):

$$Z_b = 2\mathrm{Z}_{\circ} - Z_t \qquad 3$$

Other parameters such as thermal gradient and heat flow were further estimated using the results computed from the CPD depth (Z_b).

More so, the geothermal gradient (dT/dZ) was estimated using equation 4 as (Ross *et al.*, 2006):

$$dT/dZ = \theta_c/Z_b \qquad 4$$

Where, θ_c is the Curie-temperature which depends on magnetic materials in the rock, 580^{o}C is assumed to be Curie temperature for magnetite (Fe_3O_4) will be consider as such throughout this work because magnetite is commonly abundant magnetic mineral in the crust.

Likewise, the heat flow (q_z) within the study area was estimated using equation 5:

$$Q_z = -\mathrm{k(dT/dZ)} \qquad 5$$

where *k* is thermal conductivity of different rocks type within the area of study which values were shown in (Table 1). According to Braun (2009), the conductivity of rocks increases with decrease in temperature and vice visa, this means that thermal conductivity in the lower crust is smaller than in upper or on the surface.

The negative sign in heat flow equation (equation 5) indicates the direction of flow of heat which moves in the opposite direction to the depth of the source.

Acquisition and processing of airborne radiometric data

The contribution of radio- elements such as Uranium (U), Thorium (Th) or Potassium (K) to the earth's interior heat is much common in crustal rocks. Moreover, aero-radiometric data were obtained and gridded to determine the concentration of each radio-element within the study area.

Estimation of Radioactive Heat Production

The most prominent isotope decay series which are common in rocks are thorium series (^{232}Th), decay of the potassium isotope (^{40}K) and uranium series (^{238}U and ^{235}U). So, radioactive heat production (HTP) was determined by substituting values of each of the radioelement content of the gridded aero-radiometric data in equation 6 as shown in Rybach (1988).

$$\mathrm{HTP} = 9.25Cu + 2.56Cth + 3.48Ck \quad 6$$

where, HTP is the radioactive heat production due to the concentration of uranium and thorium (in ppm), and potassium (in %).

Estimation of Radiogenic Heat Generation

The radiogenic heat generation (Rg) in μWm^{-3} produced due to the concentrations of potassium, uranium, and thorium using the computed values of radioactive heat production and multiplying by the density of rock types in the area as shown in equation 7 (Rybach, 1988).

$$\mathrm{Rg} = 10^{-5}\rho\mathrm{HTP} \quad 7$$

where ρ is density of the rock (in kgm^{-3}) and HTP is the radioactive heat production. The values of radiogenic heat were computed and used to produce the map of radiogenic heat generation.

Variation of Temperature with Depth

A model was derived to determine the variation of temperature with depth within the area of study using the solution to 1- Dimensional heat flow equation as shown in equation 8.

$$T_d = T_o + \frac{q_s d}{k} + \frac{A_s c(c-d)}{k} - \frac{A_s c^2 exp(-d/c)}{k} \quad 8$$

where; q_s is heat flow obtained from the magnetic data, T_o surface temperature, c is the empirical heat production depth distribution parameter assumed to be 10 km, (Ravat *et al.*, 2016) and k is thermal conductivity of the rock type (Table 1), T_d is Temperature at d-depth (variation of temp-with-depth) and A_s radiogenic heat generation.

RESULTS AND DISCUSSION

The results of this study were computed from the following:

Interpretation of Magnetic Data

The values in table 2 present results of the estimated parameters from all the 17 blocks of the gridded aeromagnetic data. The depths to the top and centroid of the magnetic sources were estimated using spectral analysis method (see figure 4). It was gathered that the values of depths to the top range between 0.62 and 3.60 km with a mean value of 2.11 km. Likewise, the values of depths to the centroid of the range between 4.28 and 6.76 km with a mean value of 5.52 km. Also, the values of the CPD range between 5.0 and 12.50 km with a mean value of 8.75 km.

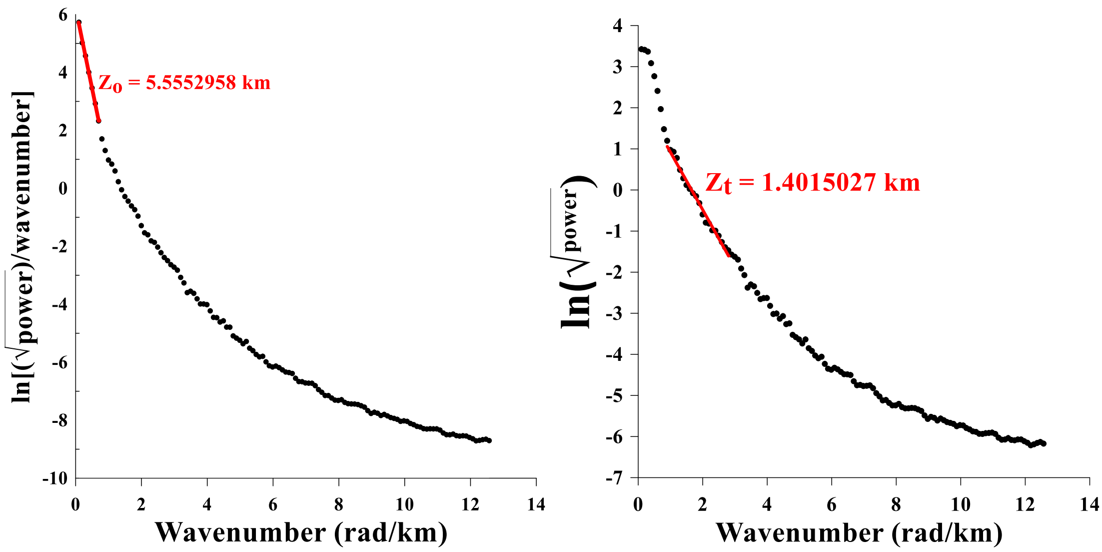

Figure 4: graph of Spectral plot of block 31.

Table 2: computed values of the parameters analyzed within the area of study.

BLOCK No	Rocks Types	Z_t (km)	Z_o (km)	CPD (km)	Geothermal gradient (^{o}Ckm^{-1})	Heat Flow (mWm^{-2})	Lat	Long
1.	Alluvium	2.10	5.40	8.70	66.70	166.75	4.25	13.75
2.	Alluvium	1.98	5.11	8.24	70.38	175.96	4.75	13.75
3.	Dolorite	1.70	5.31	8.92	65.03	162.56	5.25	13.75
4.	Shale	1.50	4.91	8.32	69.74	174.35	5.75	13.75
5.	Limestone	3.60	4.28	4.96	116.86	292.14	6.25	13.75
8.	Alluvium	1.61	4.75	7.88	73.56	183.91	4.25	13.25
9.	Shale	1.50	4.35	7.20	80.58	201.46	4.75	13.25
10.	Shale	1.52	4.72	7.92	73.24	183.10	5.25	13.25
11.	Granite	1.23	4.46	7.70	75.36	188.40	5.75	13.25
12.	Granite	1.05	5.35	9.65	60.14	150.34	6.25	13.25
13.	Granite	0.67	5.17	9.68	59.93	149.83	6.75	13.25
27.	Schist	1.56	6.24	10.93	53.07	132.69	4.25	12.75
28.	Migmatite	1.52	5.78	10.04	57.76	144.39	4.75	12.75
29.	Granite	1.40	5.52	9.64	60.15	150.37	5.25	12.75
30.	Alluvium	1.02	6.76	12.50	46.39	115.98	5.75	12.75
31.	Alluvium	1.40	5.56	9.71	59.74	149.34	6.25	12.75
32	Alluvium	0.62	4.29	7.95	72.92	182.30	6.75	12.75

Figure 5 is the CPD map of the study area which reveals two distinctive zones of varying Curie depths. These include shallow and deep CPD zones.

The shallow CPD zones have values ranging from 5.0 to 8.70 km which dominate almost the entire northern parts, covering places such as Kurdula, Wurno and Kaura Namoda areas respectively.

The deep CPD zones with values ranging from 9.0 and 12.50 km in the South, SW and SE boundaries which sweep through the central area including; Talata Mafara, Argungu, Gulma, Shinkafe, Moriki, Sokoto and Maradun.

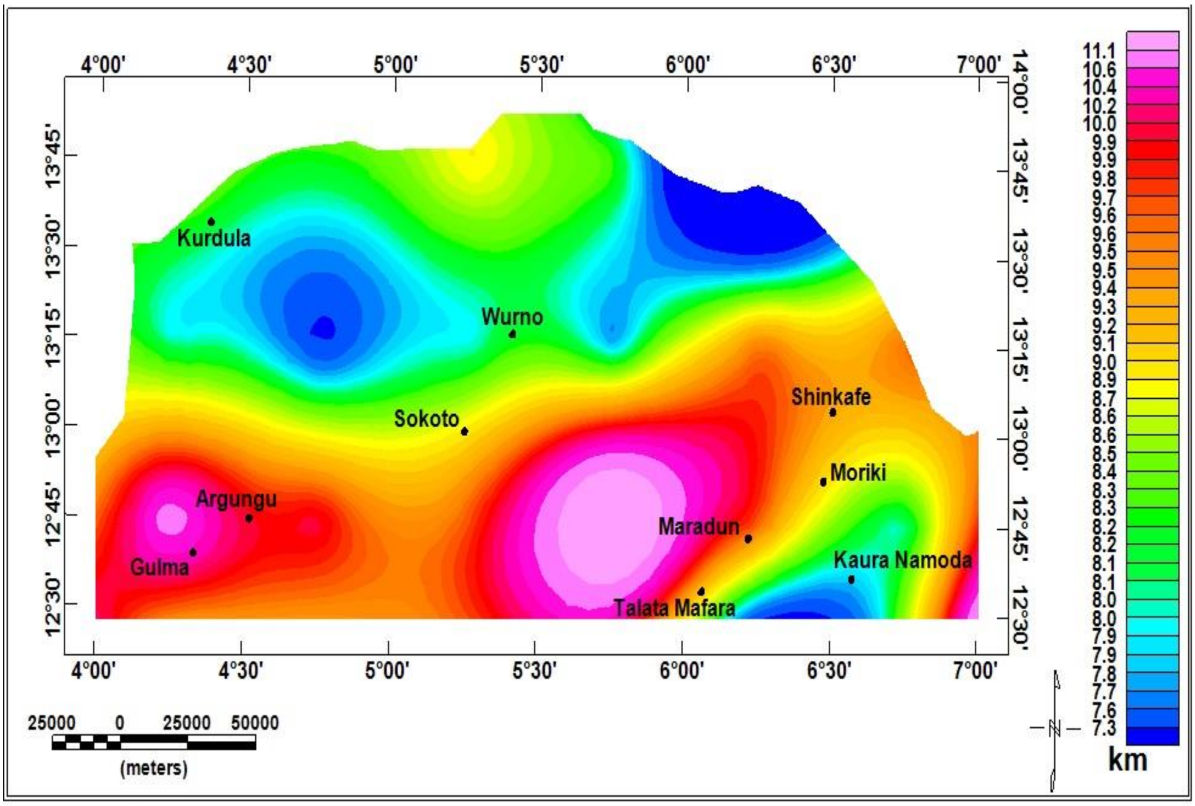

Figure 5: showing Map of CPD of the area of study.

Figure 6 shows the geothermal gradient map of the study area which was produced using the values of geothermal gradient in table 2. The result reveals that the values range between 46.39 and 116.86 ^{o}C/km with a mean value of 81.63 ^{o}C/km. This map reveals two dissimilar spots of varying geothermal gradient which are the high and low geothermal gradient.

The high geothermal gradient values range between 70.6 and 116.86 ^{o}C/km covering the majority parts of the north with pocket in the southern boundary that include; Kurdula, Wurno and Kaura Namoda respectively.

The low geothermal gradient values range between 46.39 and 68.4 ^{o}C/km in the SE, SW and south boundaries through the central parts to include; Talata Mafara, Argungu, Gulma, Shinkafe, Moriki, Sokoto and Maradun.

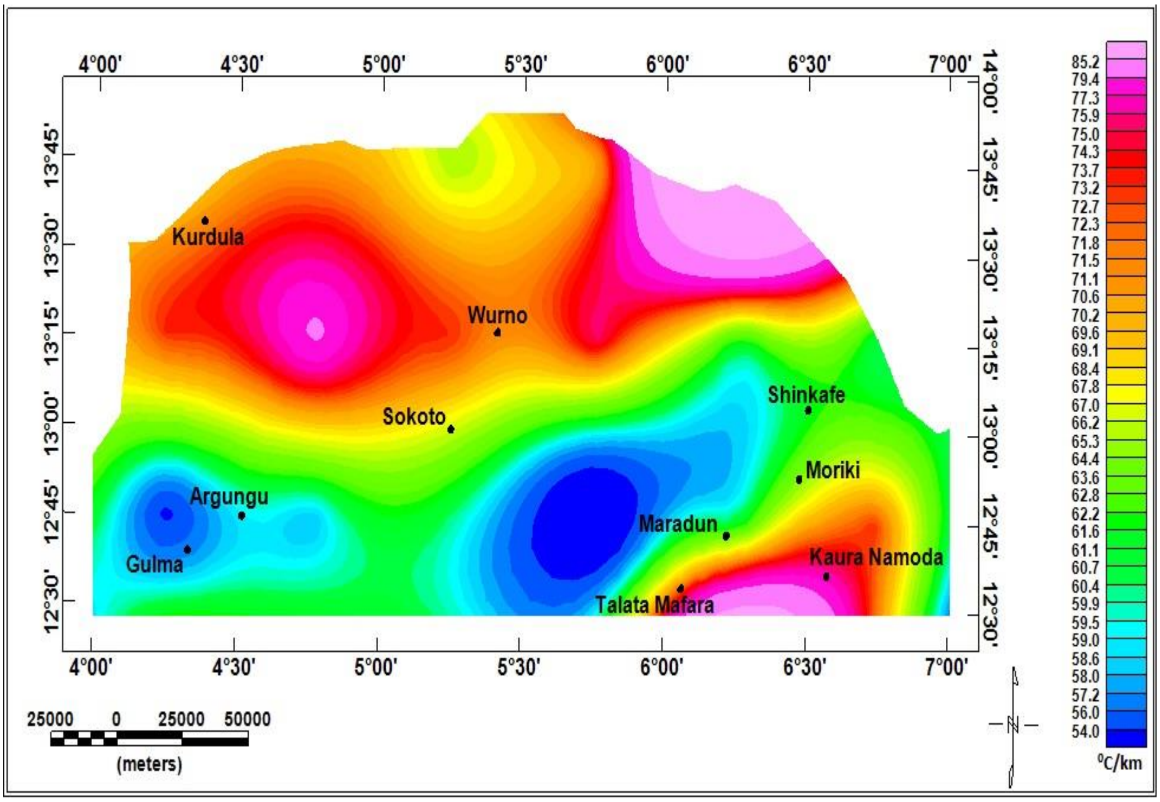

Figure 6: showing Map of geothermal gradient of the area of study.

Figure 7 shows the heat flow map of the study area. The result reveals that the values of heat flow range between 115.9 and 292.14 mWm^{-2} with a mean value of 204.06 mWm^{-2}. From this map, the area can be categorized into the low and high heat flow zones.

The Low heat flow have values ranging from 115.9 to 147.8 mWm^{-2} in NW, central parts and SW boundary that include Argungu, Gulma Maradun, Sokoto and Kurdula.

Similarly, zones with high heat flow values ranging from 151.4 and 292.14 mWm^{-2} in the NE, NW, North and Southern border sides including places like Wurno, Shinkafe, Moriki, Kaura Namoda, and Talatu Mafara.

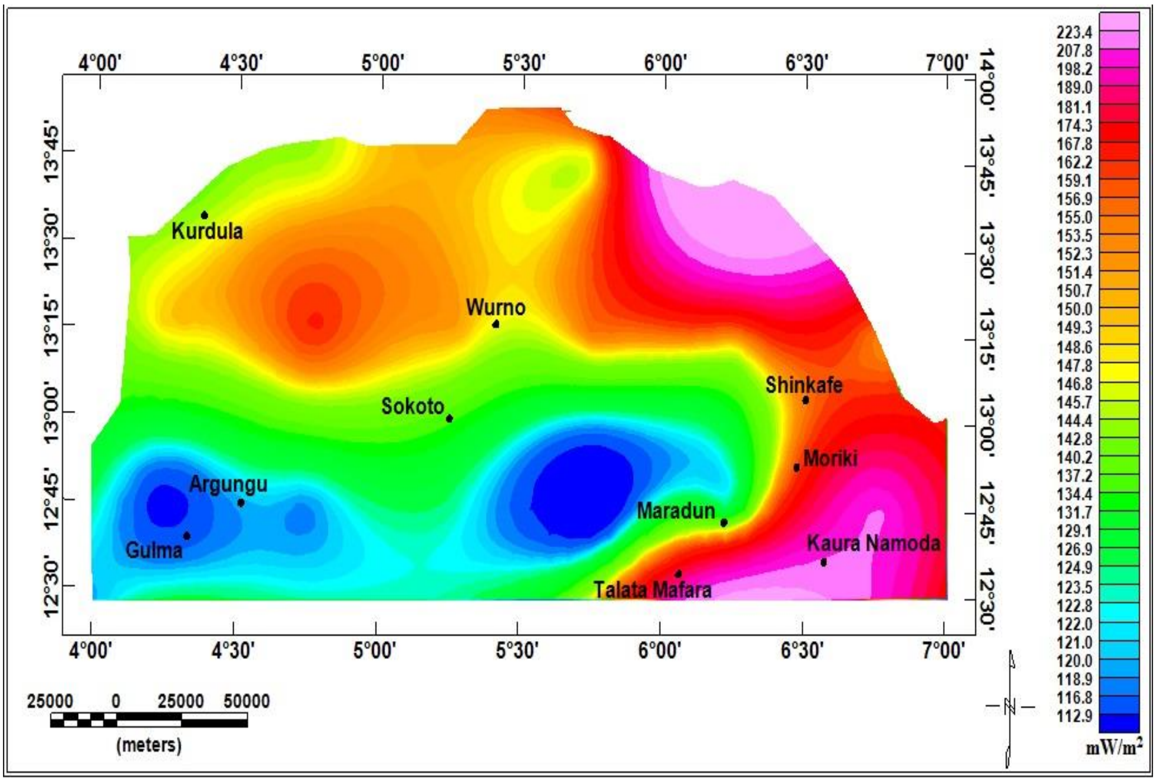

Figure 7: showing Map of Heat flow of the area of study.

Interpretation of Radiometric Data

In order to present a plain result of this analysis, the work therefore estimates the radiogenic heat generation using aero-radiometric data of the study area.

Figure 8 reveals high concentration of potassium (K) in SE part with values range between 0.23 and 1.96 % while low values of K concentration dominated almost the area with range between 0.12 and 0.22 %.

Figure 9 shows high values of Thorium (Th) concentration range between 6.10 and16.91 ppm, to the North, NE, SW and SE boundaries. Likewise, low values of concentration of thorium range between 2.71and 5.95 ppm was observed in south, NE, SW and NW parts of the study area.

Figure 10 divulges high values of uranium (U) concentration range between 1.65 and 8.95 ppm, to the northern, SW boundaries and central portion scattering in all the entire area. Similarly, low values of uranium concentration range between 0.21 and 1.53 ppm dominated almost the entire locations.

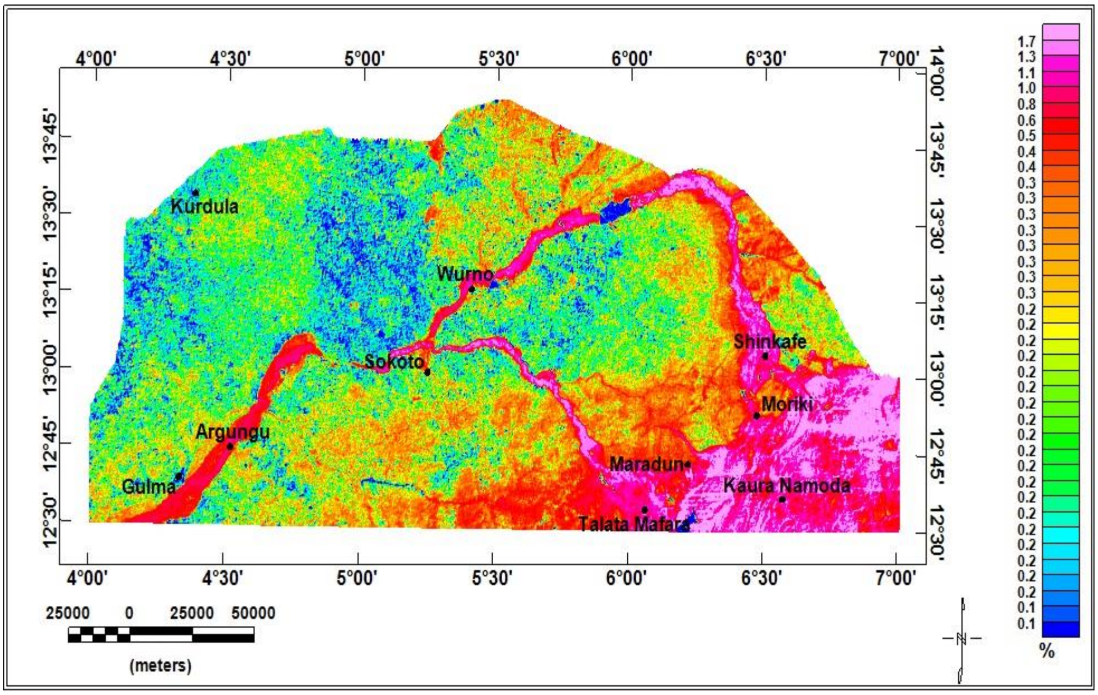

Figure 8: showing Map of concentration of Potassium (K) in the study area.

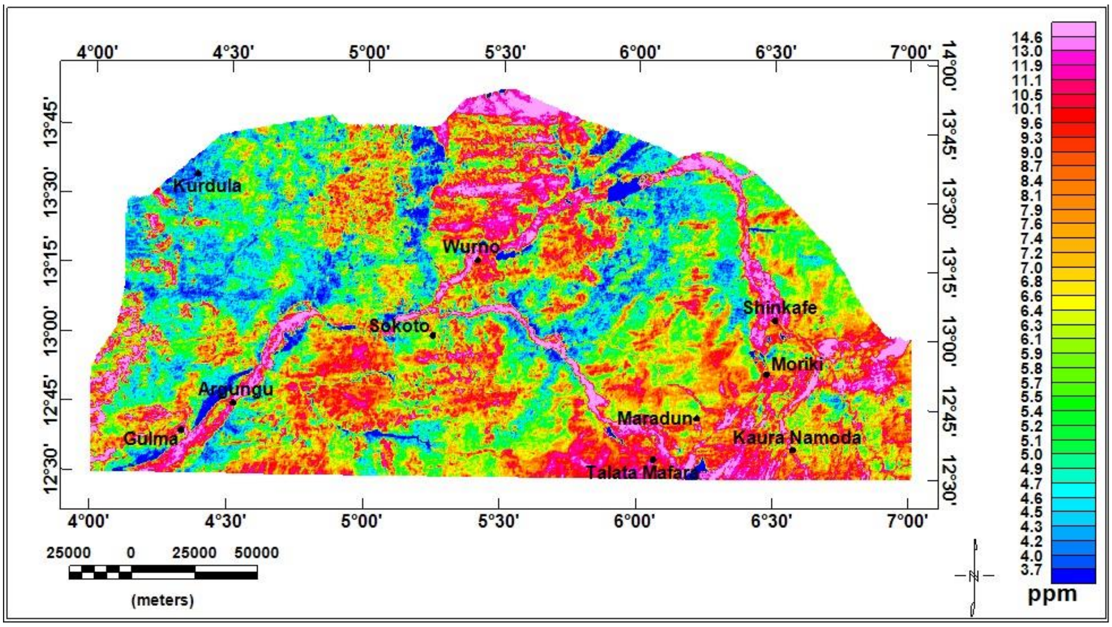

Figure 9: showing Map of concentration of Thorium (Th) in the study area.

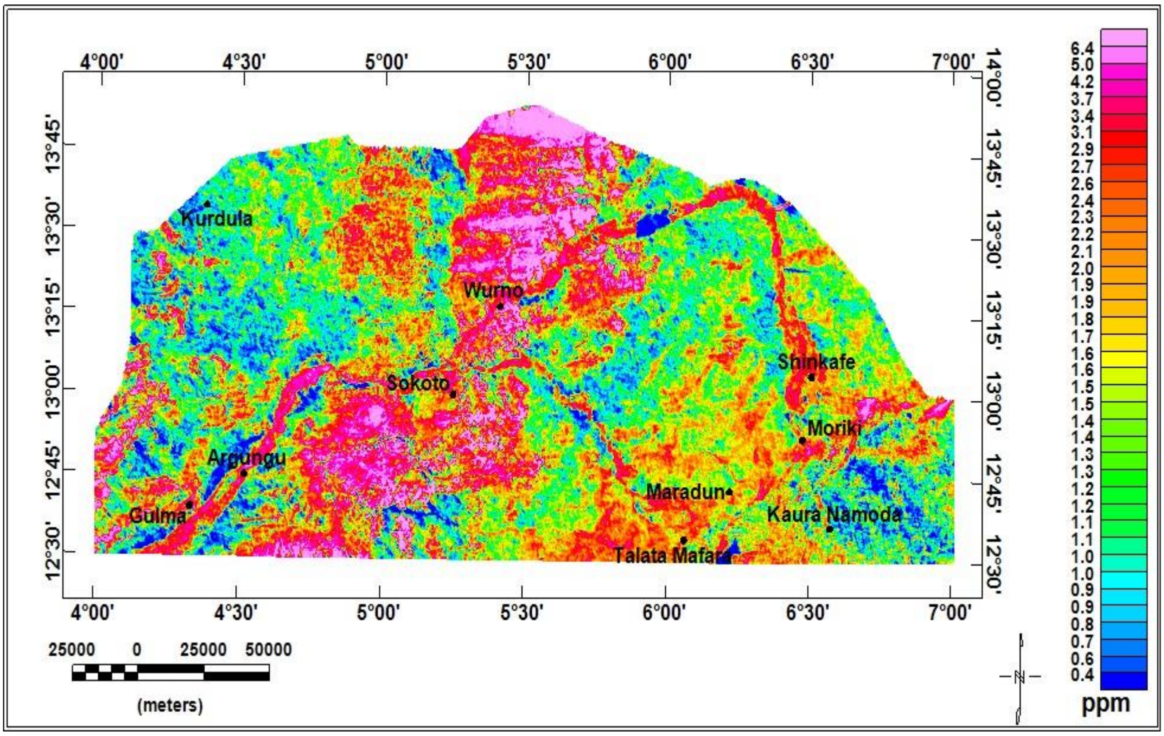

Figure 10: showing map of concentration of Uranium (U) in the study area.

Composition of radio-elements in the crust

The Ternary map presents clear pictures of the arrangement of radio-elements in the crust which appears in a form of triangular plot of the three prominent types of radio-elements. Likewise, this plot usually gives a better reflection of the geology (Salem *et al*., 2005).

Figure 11 reveals that uranium which signifies the occurrence of pegmatites and granites in dominated the area. Thus, minute quantity of potassium appear in the SE boundary implies high concentration of granite and felsic igneous basalt rocks. Similarly, thorium occupies small segment this means that the area has high concentration of mafic igneous rocks. Also, the trend of uranium and Thorium through N-S to S-W extended to Niger Republic across the mid-northern border.

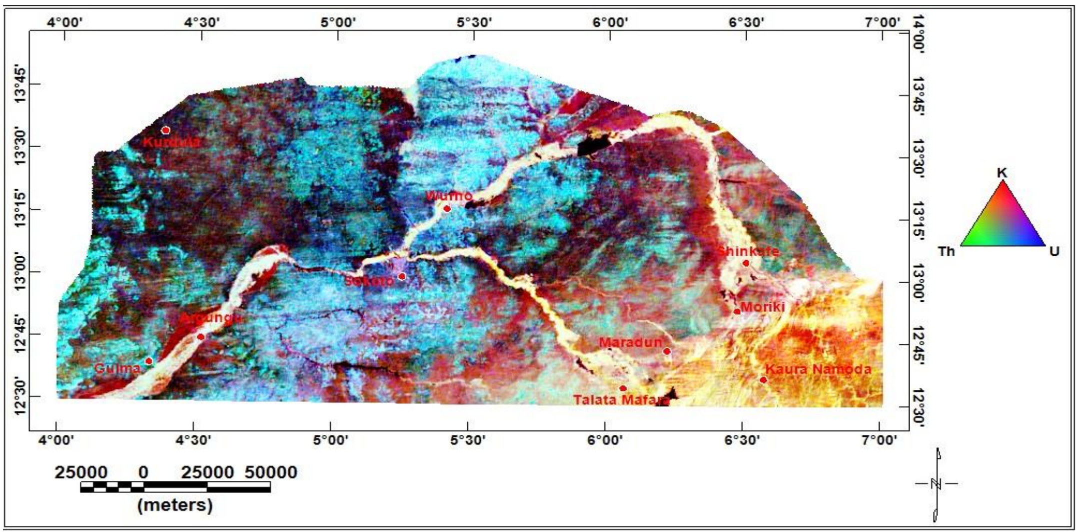

Figure 11: showing ternary Map of composition of radio-elements in the study area.

Interpretation of Radiogenic Heat Generation

Figure 12 shows high values of radiogenic heat generation range between 0.81 and 2.87 μWm^{-3} which trend from SW boundary through the central parts to the NE, north down to SE which almost dominated the entire area. Likewise, low values range between 0.78 and 0.35 μWm^{-3} in the NW and NE parts of the study area.

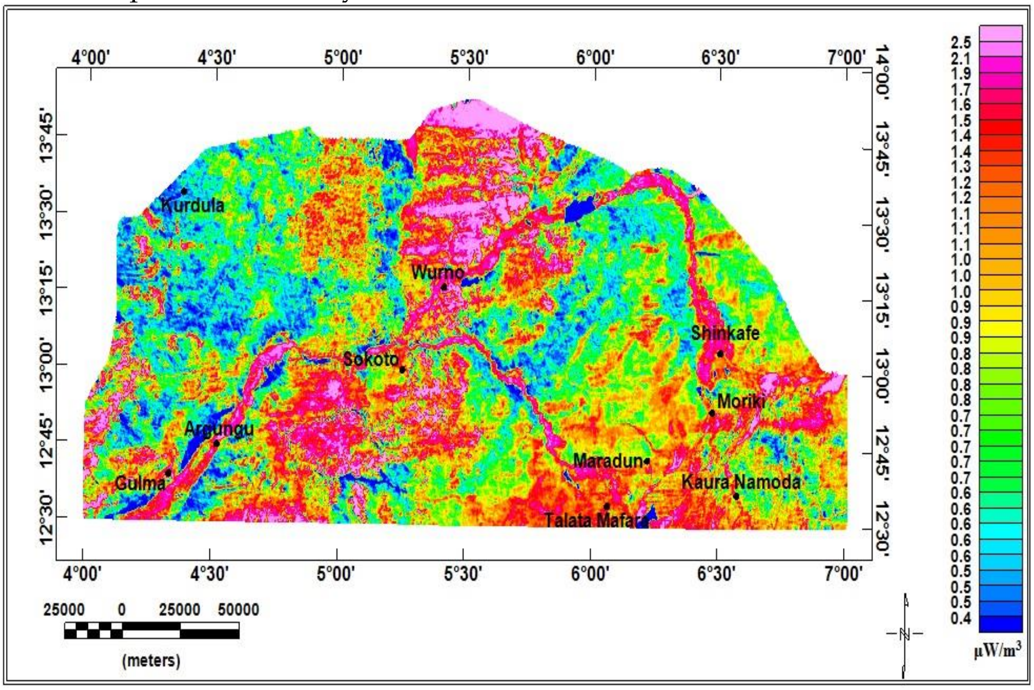

Figure 12: showing radiogenic heat generation map of the study area.

Modeling of Variation of Temperature with Depths

The estimated values of variations of temperature with depths the in the area (table 3) were computed using varying depths of 0 km, 2 km 4 km, 6 km, 8 km, and 10 km. The values were used in plotting temperature against depth graph (figure 13) showing the graphical picture of the variations. The model helps in identifying the depths to Curie temperature in the area.

Table 3: Computed values of variation of temperature with depths in the study area.

DEPTHS	0 km	2 km	4 km	6 km	8 km	10 km
	29	162.138	294.776	427.006	558.900	690.521
	28	168.380	308.078	447.218	585.902	724.211
	27.8	156.821	284.034	409.766	534.286	657.813
	27.5	165.739	301.801	436.079	568.896	700.519
	27.3	260.535	492.929	724.633	955.773	1186.452
	29	175.711	321.686	467.058	611.937	756.411
	28	188.736	348.718	508.081	666.938	825.381
TEMPERATURES	**27.8**	173.871	319.229	464.003	608.299	752.204
(°C)	**27.5**	177.889	327.698	477.033	625.978	774.605
	27.3	146.909	265.348	382.830	499.528	615.583
	26	144.803	261.742	377.155	491.319	604.460
	29	134.719	239.686	344.036	447.883	551.316
	28	142.791	256.312	368.792	480.421	591.352
	27.8	147.597	266.521	384.731	502.356	619.503
	27.5	119.753	211.078	301.643	391.586	481.020
	27.3	145.675	262.119	376.985	490.556	603.069
	26	171.058	314.742	457.300	598.937	739.819

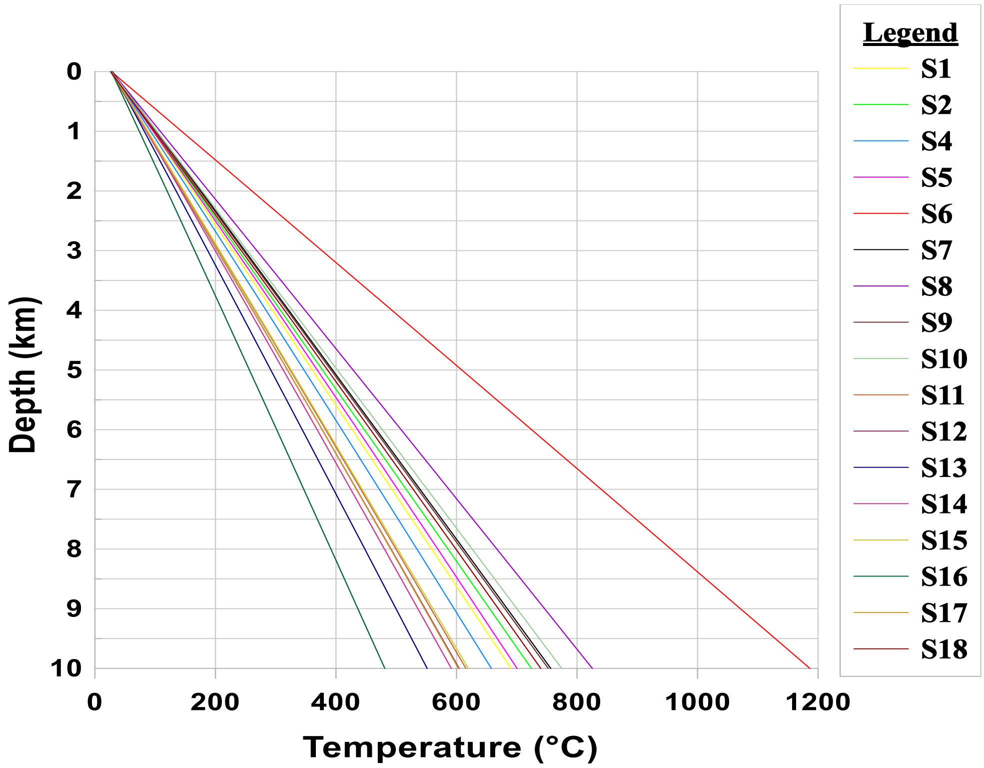

Figure 13: showing graph of variation of temperatures with depths in the study area.

DISCUSSION

The Curie point depth in the was revealed Shallow zones covering places such as Kurdula, Wurno, Kaura Namoda and a deep CPD zones which include places such as Talata Mafara, Argungu, Gulma, Shinkafe, Moriki, Sokoto and Maradun. Although, Shallow Curie isotherm depths are due to thin crust while deep CPD could be ascribe to thick crust (Yakubu *et al.*, 2022). Thus, this implies that, shallow Curie point depth indicates Crustal thinning/intrusion/updoming that may lead to the high temperature close to the surface. However, the shallow CPD regions may propose crustal thinning, whereas a deep one suggests thick crust. This, result agreed with findings from earlier work using magnetic and gravity prospective over the Sokoto Basin by Umegu (1990), which reported that the Basin is generally shallow and that the underlying Basement rocks are gently folded.

The geothermal gradient of the area presents locations with high geothermal gradient in places such as Kurdula, Wurno, Kaura Namoda and locations with low geothermal gradient which include Talata Mafara, Argungu, Gulma, Shinkafe, Moriki, Sokoto and Maradun. The locations with deep Curie point depth matched to those with low geothermal gradient and likewise, those locations with low CPD match up with the one that have high geothermal gradient.

The heat flow of the area reveals spots with Low heat flow these are, Argungu, Gulma Maradun, Sokoto, Kurdula, these spots match up with deep CPD and low geothermal gradient zones in the area. Similarly, the high heat flow spots covering Wurno, Shinkafe, Moriki, Kaura Namoda, and Talatu Mafara, correspond to the shallow CPD and high geothermal gradient.

The heat flow of 80 mWm^{-2} to 100 mWm^{-2} indicates a viable good geothermal condition (Ludvik, 2009), however, a heat flow values greater than 100 mWm^{-2} was considered to be for anomalous geothermal condition (Jessop *et al*., 1977).

The result of this work shows that, almost all the study area present high heat flow values, >100 mW/m^2, and suggest good geothermal potential in the area.

High radiogenic heat generation range between 0.81 and 2.87 μWm^{-3} trending to SW boundary through the central parts and to the NE, north, SE which confirm the high geothermal energy potential in the area. Equally, low values range between 0.78 and 0.35 μWm^{-3} at the NE and NW.

The radiogenic heat of 2.87 μWm^{-3} reported in this study falls within the average continental crust values of radiogenic heat which is between 2.5μWm^{-3} and 2.9μWm^{-3} (Alistair *et al*., 2014; Wollenberg & Smith 1987). The high concentration zones of thorium and uranium trend in the area extends to the S-W and NS bordering Niger Republic, which also follows the path of radiogenic heat generation.

Thus, at 580°C, demagnetization occurred in a magnetite rich rocks (Salem *et al*., 2005). For hydrocarbon exploration for instance in places like Red Sea, temperature ranges between 65 and145°C for oil and 165°C for gas were reported (Staplin, 1977). Thus, in this work; Curie temperature was obtained at a minimum depth of 6 km while sedimentary maturation may perhaps occur at a minimum depth of 2 km.

CONCLUSION

This study indicates that the crust is thin within spots of shallow CPD. In the low temperature zones thermal maturation of sediments does not take place, while; high temperature zones support thermal maturation of sediments and possible oil exploitation. This work also provides thermal information that lead to the identification and utilization of geothermal energy in the area. Thus, high heat flow with a corresponding high concentration uranium/thorium and radiogenic heat generation gives the area high potential for geothermal resources that could be converted to energy source for electricity generation which will boost the power capacity in the area. Moreover, at a minimum depth of 6 km the Curie temperature might be reach within the Basin and sedimentary maturation take place at least within a depth of 2 km.

ACKNOWLEDGEMENT

The author expresses his profound gratitude to the Department of Physics Ahmadu Bello University, Zaria for the opportunity of providing guide and facilities. Also to Nigerian Geological Survey Agency (NGSA), for releasing the data used in conducting this study.

REFERENCES

Alistair, T-M, Thomas, L-H, Paul, L-Y, David, C-W & Alan, J-C 2014 'Gamma-ray Spectrometry in Geothermal Exploration': State of the Art Techniques Energies, Vol.7, 4757-4780, doi: 10.3390/en7084757.

Bhattacharyya, B-K & Leu, L-K 1975 'Analysis of magnetic anomalies over Yellowstone National Park: Mapping of Curie point isothermal surface for geothermal reconnaissance', *Journal of Geophysical Research*, Vol. 80 (32); 4461–4465, doi: 10.1029/JB080i032p04461.

Braun, J 2009 'Hot blanket in Earth's deep crust *Nature*' Vol. *458* (7236), 292–293. https://doi.org/10.1038/458292a.

Cermak, V & Rybach, L 1982 'Thermal conductivity and specific heat of minerals and rocks; handbook of terrestrial heat-flow density determination, geophysics- physical properties of rocks' pp.305-343: doi: 10.1007/10201894 62.

Ezekiel, K 2019 'Geothermal Study Over Sokoto Basin Northwestern, Nigeria': *International Journal of Engineering Science Invention (IJESI) ISSN (Online): 2319 – 6734, ISSN (Print): 2319 – 6726.*

Horai, K 1971 'Thermal conductivity of rock-forming minerals'; Journal of geophysics research, https://doi.org/10.1029/JB76i005p01278.

Jessop, A-M, Habart, M-A & Sclater, J-G 1977 'The world heat flow data collection': geothermal services of Canada Ser 50: 55.77.

Kearey, P, Brooks, M & Hill, I 2002 'An introduction to geophysical Exploration': third Edition.TJ international. pp. 2-160.

Kogbe, C-A 1981 'Cretaceous and Tertiary of the Iullemmeden Basin of Nigeria' (West Africa): Cretaceous Res, 2: 129–186.

Lúdvík, S-G 2009 'Geophysical methods used in geothermal exploration United Nations University Geothermal Training Programme Orkustofnun': Reykjavik, ICELAND *lsg@os.is*

Megwara, U-J, Udensi, E-E, Olasehinde, I-P, Daniyan, A-M & Lawal K-M 2013 'Geothermal and Radioactive Heat Studies of Parts of Southern Bida Basin', Nigeria and the Surrounding Basement Rocks; international journal of Basic and Applied Sciences 2(1)123.

NGSA 2010 'Acquisation of Aeromagnetic and Radiometric data': by Fugro airborne for Nigerian Geological Survey Agency.

NGSA 2004 'Geological map of North-western Nigeria showing the study area': for Nigerian Geological Survey Agency.

Nwankwo, L-I & Shehu, A-T 2015 'Evaluation of Curiepoint depths, geothermal gradients and near-surface heat flow using high-resolution aeromagnetic (HRAM) data of Sokoto Basin': Journal of Volcano Geothermal Research, Vol. 30 No 5, pp 45–55. https://dx.doi.org/10.4314/ijs.v23i1.17.

Obaje, N-G 2009 'Geology and Mineral Resources of Nigeria, Lecture Notes in Earth Sciences, Springer, Berlin Heidelberg.

Okubo, Y, Graf, R-J, Hansen, R-O, Ogawa, K & Tsu, H 1985 'Curie point depths of the island of Kyushu and surrounding area, Japan': *Geophysics*, Vol. 50 (3) 481–489, doi: 10.1190/1.1441926.

Olorunsola, K & Chukwu, C-G 2018 'Analysis of Geothermal Heat Flow Potentiality of Upper Bida Basin Nigeria Using Aeromagnetic Data': Int. Journal of Applied Science, 9.8. doi: 10.21767/2394-9988.100074.

Olorunsola, K & Aigbogun, C 2017 'Assessment of Aero-radiometric Data of Southern Anambra Basin for the Prospect of Radiogenic Heat Production'; Journal of Applied Science of Environ Manage, Vol. 21 (4) 743-748; https://dx.doi. org/10.4314/jasem. v21i4.15.

Quintero, W, Campos-Enriquez, O & Hernández, O 2019 'Curie point depth, thermal gradient, and heat flow in the Colombian Caribbean' (north-western South America): *7:16* https://doi.org/10.1186/s40517-019-0132-9

Ravat, D, Pignatelli, A, Nicolosi, I & Chiappini, M 2007 'A study of spectral methods of estimating the depth to the bottom of magnetic sources from near-surface magnetic anomaly data': Geophysical Journal International, Vol. 169: 421-434.

Ravat, D, Morgan, P & Lowry, A-R 2016 'Geotherms from the temperature-depth–constrained solutions of 1-D steady-state heat-flow equation Geosphre: Vol. 12, No. 4, p. 1187-1197, doi:10.1130/GES01235.1.

Rybach, K, Hokrick, R & Eugester, W 1988 'Vertical earth probe measurements and prospects in Switzerland': Communication Proc. Vol. 1, pp 67–372.

Saada, A-S 2016 'Curie point depth and heat flow from spectral analysis of aeromagnetic data over the northern part of Western Desert, Egypt': journal of Applied Geophysics, vol. 134, pp 100-111. Doi: 10.1016/j.jappgeo.2016.09.003.

Salem, A, Abouelhoda, E, Alaa, A, Atef, I, Sachio, E & Keisuke, U 2005 'Mapping Radioactive Heat Production from Airborne Spectral Gamma-Ray Data of Gebel Duwi Area, Egypt': Proceedings World Geothermal Congress, Antalya, turkey, 24-29.

Spector, A & Grant, F-S 1970 'Statistical model for interpreting aeromagnetic data': *Geophysics*, Vol. 35(2); 293–302.

Staplin, F-L 1977 'Interpretation of thermal history from colour of particulate organic matter': a Review palynology, Vol. 1 pp 9-18.

Tanaka, A, Okubo, Y & Matsubayashi, O 1999 'Curie point depth based on spectrum analysis of the magnetic anomaly data in East and Southeast Asia': *Tectonophysics,* Vol. 306(3–4); 461–470.

Umegu, M-N 1990 'Structural Interpretation of Gravity and Aeromagnetic Anomalies over Sokoto Basin, North – western Nigeria': PhD thesis, Department of Physics, Ahmadu Bello University, Zaria, Nigeria.

Wollenberg, H-A & Smith, A-R 1987 'Radiogenic heat production of crustal rocks: An assessment based on geochemical data': Geophysical Research Letters, Vol. 14, pp 295–298, doi: 10 .1029 /GL014i003p00295.

Yakubu, M-B, Lawal, K-M, Dewu, B-B-M & Ikpokonte, A-E 2022 'Investigation of geothermal energy resource potential using aeromagnetic and aero-radiometric data of Kano, Nigeria'; fudma journal of sciences ISSN online: 2616-1370; Vol.6 No.1 pp 296-307.